Supplementary Information (SI) for Physical Chemistry Chemical Physics.
This journal is © the Owner Societies 2026

SUPPORTING INFORMATION

Three-dimensional electric double layer at solvent-free liquid/liquid interface between two immiscible ionic liquids

Kazuma Yamaguchi[1], Kazuya Kobayashi[1], Kosuke Ishii[2], Yishan Zhou[1], Yuko Yokoyama[1], Tetsuo Sakka[1] and Naoya Nishi[1]

[1]*Graduate School of Engineering, Kyoto University, Kyoto 615-8510, Japan,*

[2]*High Energy Accelerator Research Organization, Ibaraki 319-1106 Japan,*

**Corresponding author: Naoya Nishi: nishi.naoya.7e@kyoto-u.ac.jp*

S1. Force field of $TOMA^+$

The N atom, the α- and β-position C and H atoms of the methyl and octyl groups of $TOMA^+$ were described using the force field of CL&P[1, 2]. The C and H atoms from the γ-position onward were modeled using the force field of Jorgensen et al. in 2024[3]. C* and represents CA, CM, C2, CS, and CT. H* represents either HM or HC.

Fig. S1 Nomenclature of $TOMA^+$.

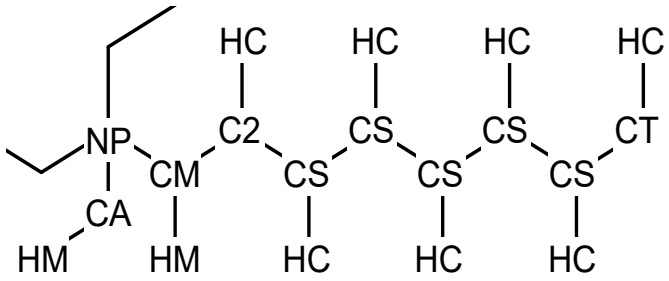

Table S1 Atom parameters of $TOMA^+$. The van der Waals potential was described by Lennard-Jones potential, $4\varepsilon\{(\sigma/r)^{12} - (\sigma/r)^6\}$.

atom	q / e	σ / nm	ε / kJ mol^{-1}
NP	0.096	0.325	0.71128
CM, CA, C2	-0.136	0.350	0.27614
C2	0.008	0.350	0.27614
CS	-0.096	0.350	0.27614
CT	-0.144	0.350	0.27614
HM	0.104	0.250	0.12552
HC	0.048	0.250	0.12552

Table S2 Bond parameters of $TOMA^+$. The bond potential was described by harmonic oscillator potential, $(k_r/2)(r - r_0)^2$.

bond	r_0 / nm	k_r / kJ mol^{-1} nm^{-2}
NP-C*	0.1471	307100
C*-C*	0.1529	224000
C*-H*	0.1090	constraint

Table S3 Angle parameters of $TOMA^+$. The angle potential was described by harmonic oscillator potential, $(k_\theta/2)(\theta - \theta_0)^2$.

angle	θ_0 / deg	k_θ / kJ mol^{-1} deg^{-2}
C*-NP-C*	109.5	418.4
NP-C*-H*	109.5	209.2
NP-C*-C*	109.5	669.4
C*-C*-C*	112.7	488.6
C*-C*-H*	110.7	314
H*-C*-H*	107.8	280

Table S4 Dihedral parameters of $TOMA^+$. The dihedral potential was described by OPLS potential, $\sum_{m=1}^{4}(V_m/2)\{1 + (-1)^{m+1}\cos(m\phi)\}$.

dihedral	V_1 / kJ mol^{-1}	V_2 / kJ mol^{-1}	V_3 / kJ mol^{-1}	V_4 / kJ mol^{-1}
NP-CM-C2-HC	-4.2384	-2.9665	1.9790	0.0000
NP-CM-C2-CS	10.0081	-2.8200	2.3012	0.0000
C*-NP-CM-C2	1.7405	-0.5356	2.9079	0.0000
C*-NP-C*-H*	0.0000	0.0000	2.3430	0.0000
C*-C*-C*-C*	3.5600	-0.8370	0.8370	0.0000
C*-C*-C*-H*	0.0000	0.0000	1.2600	0.0000
H*-C*-C*-H*	0.0000	0.0000	1.2600	0.0000

S2. Compositions in the system

Table S5 Compositions in the system. The concentration of the aqueous solution was set to 0.56 mol/L for both W phases.

	IL/IL interface	IL/W interface	
		W(EAN)	W($LiNO_3$)
$TOMA^+$	200	200	200
$C4C4N^-$	200	200	200
EA^+	2000	100	0
Li^+	0	0	100
NO_3^-	2000	100	100
water	0	10000	10000

S3. Experimentally confirmed polarizability at the IL/IL interface

S3.1. Synthesis

The hydrophilic IL, EAN, was prepared by mixing ethylamine (70 wt% aqueous solution, TCI) and nitric acid (60wt% aqueous solution, FUJIFILM Wako)[4], while the hydrophobic IL, TOMAC4C4N, was prepared from $[TOMA^+]Cl^-$ and $Li^+[C4C4N^-]$[5]. $[TOMA^+]Cl^-$ was synthesized by the dropwise addition of a dichloromethane solution of methyl chloroformate (TCI) to a dichloromethane solution of trioctylamine (TCI) under an ice-cooling condition. EAN was purified by freeze-drying, and TOMAC4C4N was purified by column chromatography and freeze-drying.

S3.2. Electrochemical measurement

A micropipette with a tip inner diameter of 20 μm was prepared, Ag/AgCl wires were used as quasi reference electrodes (QREs) in the EAN and TOMAC4C4N phases, according to the procedure described in the reference[4]. Cyclic voltammograms (CVs)

were recorded using a two-electrode cell in Fig. S2. The data were corrected by subtracting the *IR* drop with a solution resistance of 150 MΩ. A CV in Fig. S3 shows that

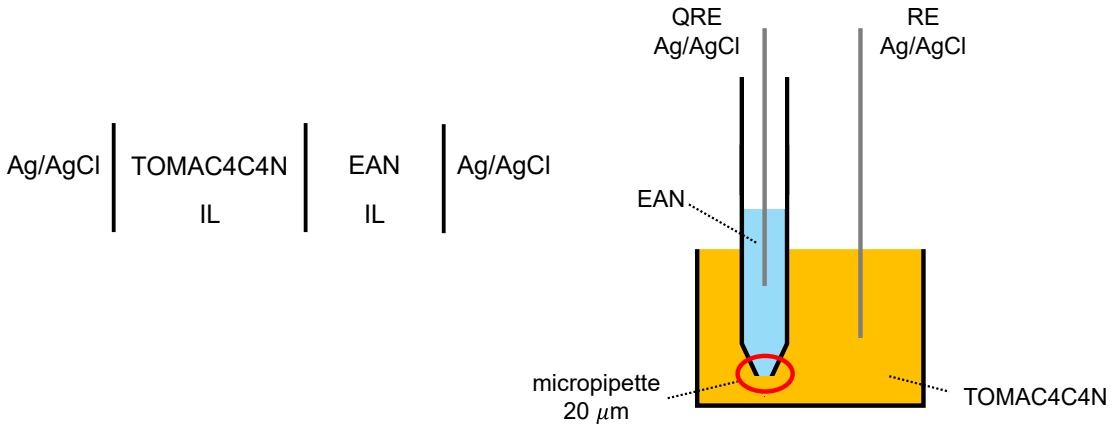

Fig. S2 Cell diagram (left) and schematic of the 2-electrode cell for recording CVs (right) at the TOMAC4C4N/EAN interface.

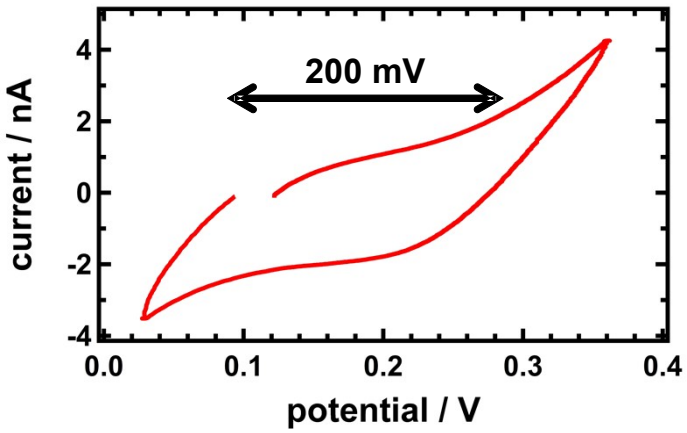

Fig. S3 Cyclic voltammogram at the TOMAC4C4N/EAN interface. The potential window width is 200 mV. The sweep rate was 0.1 V/s.

the TOMAC4C4N/EAN interface was polarizable with a potential window of 200 mV.

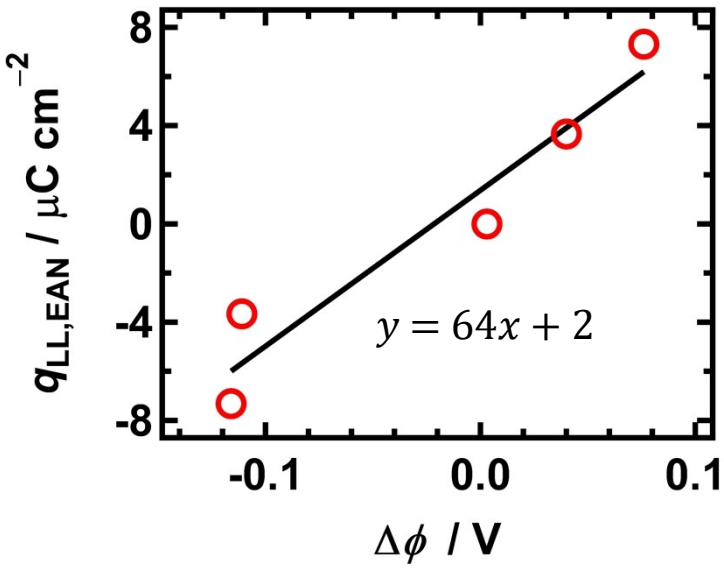

Fig. S4 Relationship between the surface charge density $q_{LL,EAN}$ and interfacial potential difference $\Delta\phi$, MD data (red open circle) and linear approximation (black solid line).

S3. Capacitance at the IL/IL interface

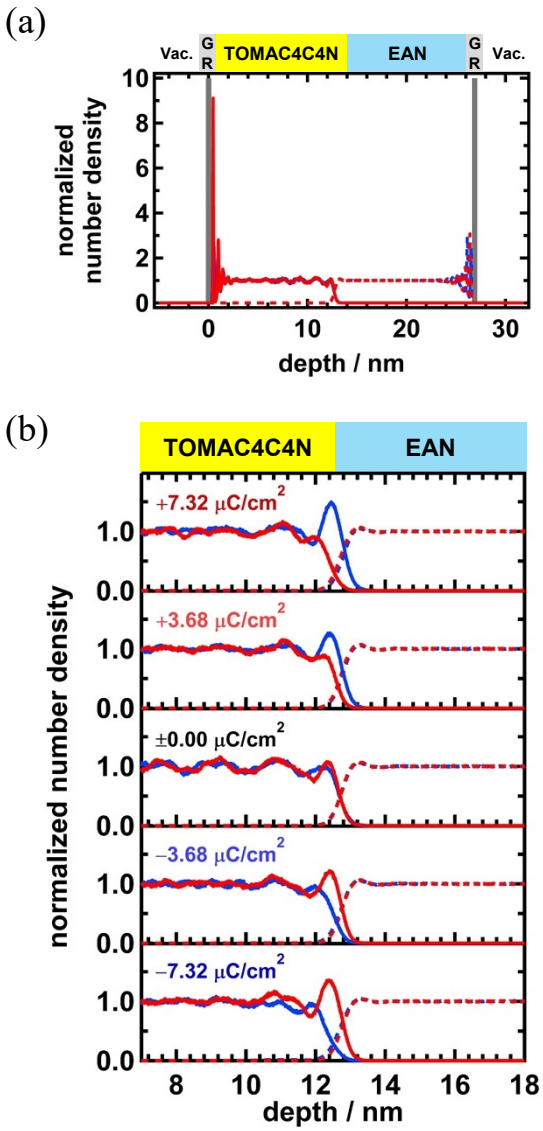

Fig. S5 Number density distribution along the z axis (a) for overall in the system at $q_{GR,EAN} = 0.00\ \mu$C/cm^2, and (b) at the IL/IL interface at various $q_{GR,EAN}$; the N atom of $TOMA^+$ (red), $C4C4N^-$ (blue), EA^+ (red dashed), and NO_3^- (blue dashed).

S4. Number density distribution at the IL/IL interface

S5. Relationship between the surface charge density of accumulated ions and q_{GR} in the magnitude

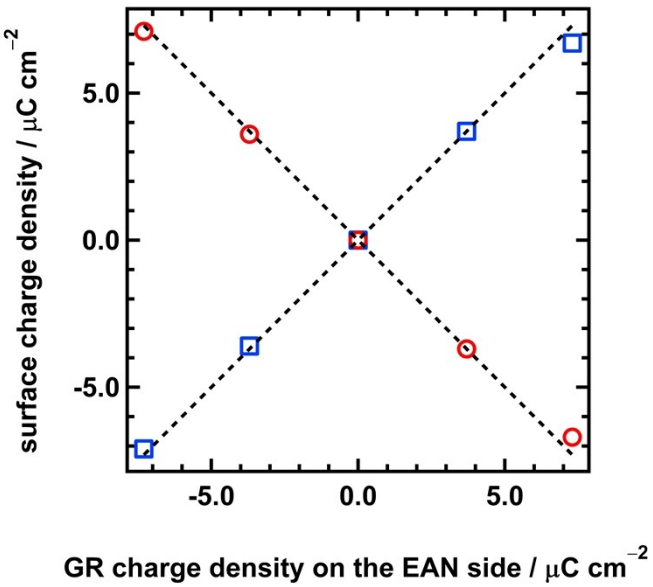

Fig. S6 Surface charge density of accumulated ions on the TOMAC4C4N (red open circle) and EAN (blue open square) sides of the IL/IL interface as a function of q_{GR}. The surface charge density of accumulated ions was evaluated by integrating the charge density peaks in Fig. 5 from z = 10 to 15 nm. The dashed lines are $y = \pm x$.

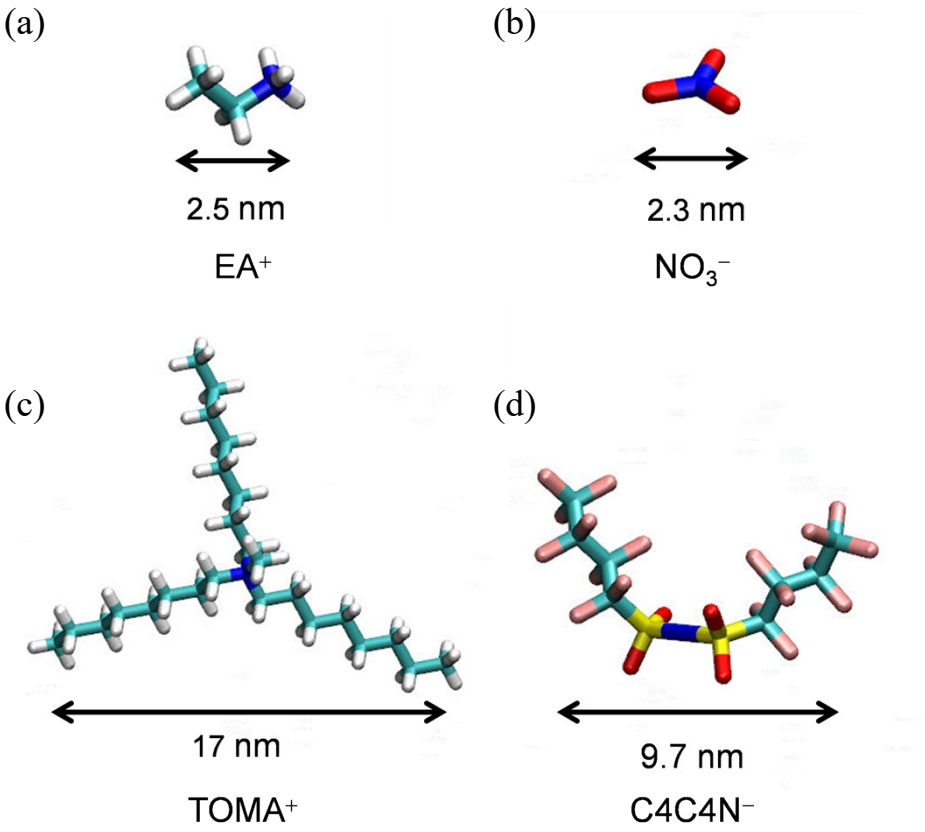

Fig. S7 Ionic size in the system. The double-ended arrows represent the distances between (a) the N atom and the terminal C atom of the ethyl group in EA^+, (b) the two O atoms in NO_3^-, (c) the two terminal C atoms of the octyl groups in $TOMA^+$, and (d) the two terminal C atoms of the perfluorobutyl groups in $C4C4N^-$.

S6. Ionic size in the system

S7. Charge density distribution at the IL/W interface

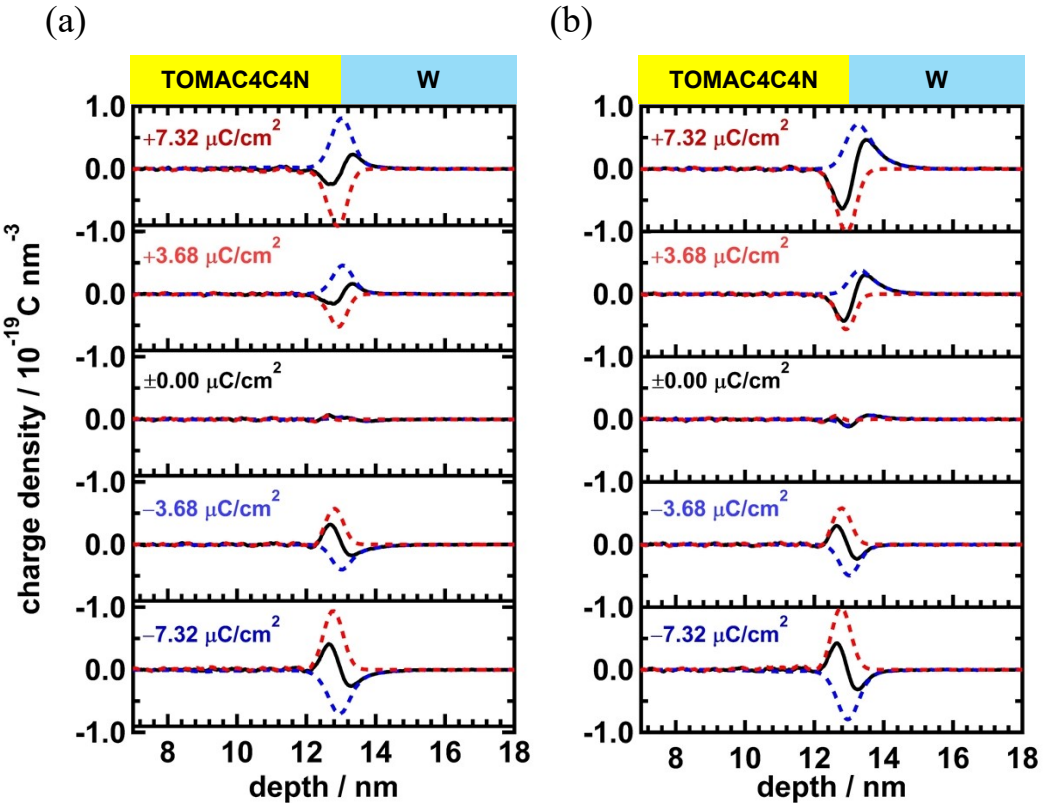

Fig. S8 Charge density distribution along the *z*-axis at the (a) TOMAC4C4N/W(EAN) and (b) TOMAC4C4N/W($LiNO_3$) interface for (black) total ions in the system, (red) ions in the TOMAC4C4N phase, (blue) ions in the hydrophilic phase.

S8. Interfacial roughness at each system

(a)

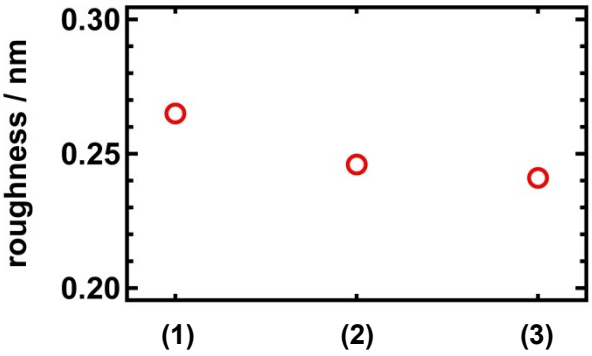

(b)

$$\rho_{\text{total atoms}}(z) = \frac{\text{a}}{1 + \text{erf}\{-\text{b}(z - \text{c})\}}$$

$$\text{roughness} = \frac{1}{\sqrt{2}\text{b}}$$

Fig. S9 (a) interfacial roughness at the (1) TOMAC4C4N/EAN, (2) TOMAC4C4N/W(EAN), and (3) TOMAC4C4N/W($LiNO_3$) interfaces at $q_{GR,EAN}$ = 0.00 μC cm^{-2}, and (b) the fitting function used to evaluate the interfacial roughness.

S9. Distance of the first coordination shell of NO_3^- around the $TOMA^+$

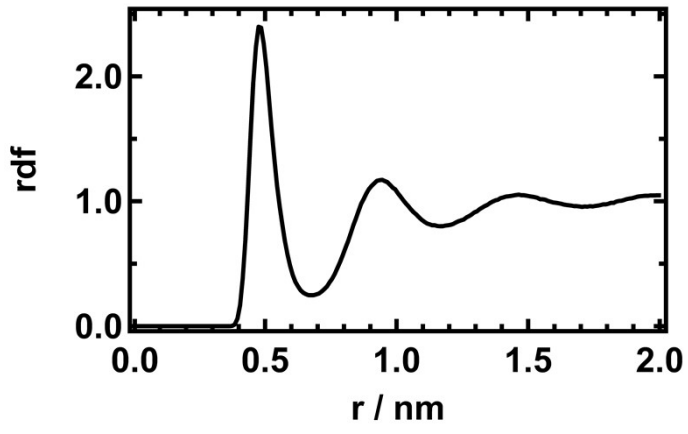

Fig. S10 RDF of the N atom of NO_3^- around the N atom of $TOMA^+$ at the (a) TOMAC4C4N/EAN interface. The boundary of the first and second coordination shells of NO_3^- was at 0.67 nm.

S10. Interfacial region at the polarizable interface

To calculate the RDF around a center atom at the interface, atoms whose positions are in the interfacial region (z) were selected. The interfacial region was defined as the full width at half maximum obtained by fitting the two peaks of the charge density distribution at $q_{GR} = \pm 3.68\ \mu C/cm^2$ (Fig. 5) with Lorentzian functions (Fig. S11). The interfacial regions (z) at the three interfaces are shown in Table. S6.

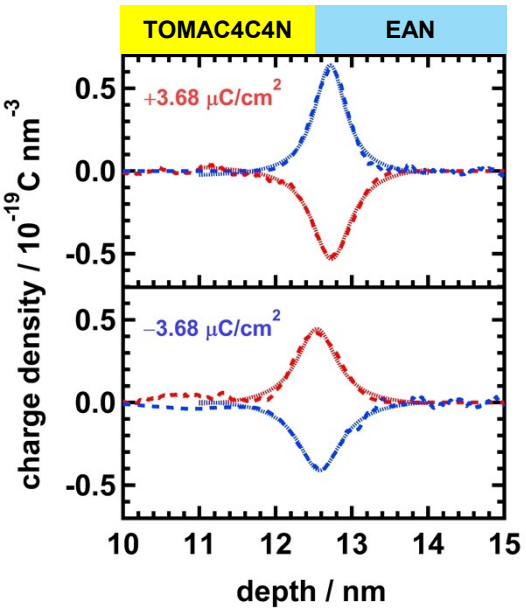

Fig. S11 Fitting the peaks of the charge density distribution at the IL/IL interface. The peaks from MD data (dashed line) and fitting Lorentzian functions (solid line).

Table S6 Interfacial regions at the three interfaces.

Interface	Interfacial region (z) / nm
IL/IL	12.33 ~ 12.95
IL/W(EAN)	12.67 ~ 13.23
IL/W($LiNO_3$)	12.74 ~ 13.31

S11. EDL structure at the liquid/liquid interface

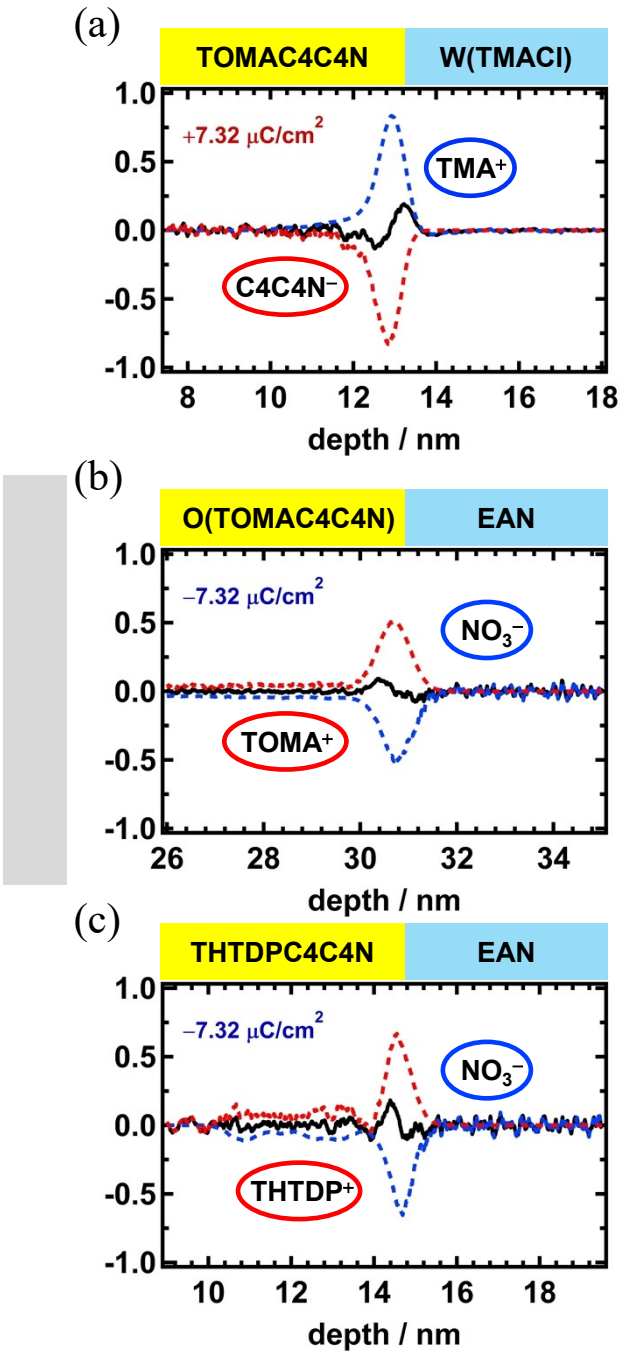

Fig. S12 Charge density distribution along the z-axis at the (a) IL/W{TOMAC4C4N/W(TMACl)}, (b) O/IL{Toluene(TOMAC4C4N)/EAN}, and (c) IL/IL{THTDPC4C4N/EAN} interface at $q_{GR,EAN}$ for (black) total ions in the system, (red) ions in the hydrophobic phase, and (blue) ions in the hydrophilic phase.

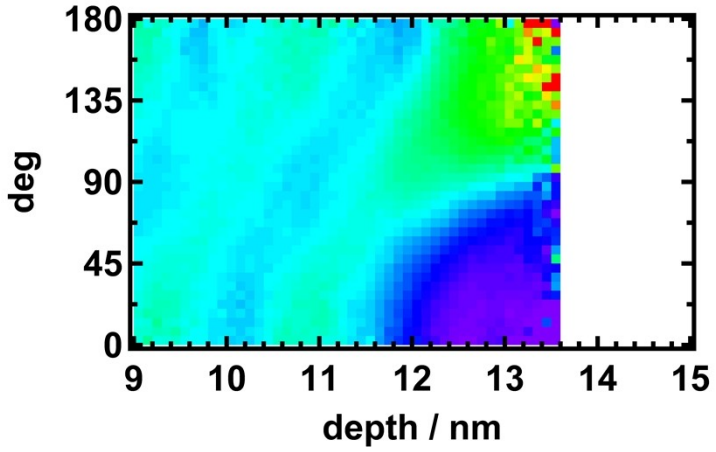

Fig. S13 Two-dimensional mapping of the orientational angle distribution along the *z*-axis for the N-$C_{perfluorobutyl}$ vectors of $C4C4N^-$.

S12. Orientational correlation dependence of $C4C4N^-$

Reference

[1] J. N. Canongia Lopes and A. A. H. Pádua, J. Phys. Chem. B, 108, 16893 (2004).

[2] J. N. Canongia Lopes and A. A. H. Pádua, J. Phys. Chem. B, 110, 19586 (2006).

[3] W. L. Jorgensen et al., J. Phys. Chem. B, 128, 250 (2023).

[4] K. Miyazato et al., J. Electroanal. Chem., 954, 118038 (2024).